Continuous Phase Transformation in Nanocube Assemblies

Yugang Zhang,[1] Fang Lu,[1] Daniel van der Lelie,[2,*] and Oleg Gang[1,†]

[1]*Center for Functional Nanomaterials, Brookhaven National Laboratory, Upton, New York 11973, USA*
[2]*Biology Department, Brookhaven National Laboratory, Upton, New York 11973, USA*

(Received 26 February 2011; revised manuscript received 9 June 2011; published 21 September 2011)

The phase behavior of 3D assemblies of nanocubes in a ligand-rich solution upon solvent evaporation was experimentally investigated using small-angle x-ray scattering and electron microscopy. We observed a continuous transformation of assemblies between simple cubic and rhombohedral phases, where a variable angle of rhombohedral structure is determined by ligand thickness. We established a quantitative relationship between the particle shape evolution from cubes to quasispheres and the lattice distortion during the transformation, with a pathway exhibiting the highest known packing.

DOI: 10.1103/PhysRevLett.107.135701 PACS numbers: 64.75.Yz, 73.22.−f, 81.05.−t, 81.07.−b

The phase behavior of self-assembled molecularly stabilized and mediated spherical nanocolloids has been an active area of research [1–3]. Recent advances in the fabrication of anisotropic shaped particles allow for an exploration of geometrical effects in their condensed phase [4,5]. On the nanoscale, the packing behavior of ligand-tethered objects, such as cubes [6] and polyhedrons [7,8], can deviate significantly from the pure geometrical predictions due to the contribution of soft molecular shells via modulation of particle shape and interparticle interactions. The resulting interplay between geometrical effects and shell properties provides a conceptually new parameter for nanocolloid assembly. Furthermore, free ligands in a solution can also play crucial roles for assembly of condensed states. For instance, ligand excess favored the ordering of 2D spherical colloidal arrays [9], whereas it induced a phase separation for particles with different shapes [10].

In addition to assembly of static systems, an investigation of reorganization in systems built from reconfigurable components is imperative for smart and stimuli-responsive materials. Recently, several studies reported transformations in systems containing molecular decorated reconfigurable objects, such as length-switchable rod assemblies [11] and molecularly stimulated 3D nanoparticle arrays [12]. From a fundamental perspective, the relationship between a structurally evolving single component and the resulting structural response of the whole system is not well understood, partially due to limited experimental realizations. Here, we adopted dodecanethiol (DT) ligated palladium nanocubes (NC) as a model for investigation of a phase behavior of NCs' 3D assembly during the system reconfiguration process. We observed a continuous structural transformation of NC assemblies in a ligand-rich solution during solvent evaporation. The changes were attributed to the evolution of particle shape from a cube to a quasisphere.

The studied system consists of well-defined palladium cubes with an edge of 10.6 ± 0.9 nm [Fig. 1(a)]. NCs were synthesized in an aqueous solution by a modified procedure [13] using polyvinylpyrrolidone (PVP) capping and subsequently replaced by a DT ligand [inset of Fig. 1(b)] with thickness ~1.7 nm [14]. High-resolution transmission electron microscopy (TEM) reveals a face-centered-cubic- (fcc-)type single crystal of NC [inset of Fig. 1(a)]. We conducted the synchrotron-based small-angle x-ray scattering (SAXS, NSLS X-9A beam line, $\lambda = 0.7867$ Å) measurements of NCs dispersed in aqueous solution [Fig. 1(b)]. The fit (IRENA package [15]) of an angular averaged SAXS profile yields a spherical particle whose volume corresponds to a cube with a 10.9 nm edge length, that is in agreements with TEM results. We induced assembly of DT-coated NCs by placing them into a slightly poor solvent, toluene (40 μl) at ~5% of solid content. The effect of free ligands on the assembly was studied by adding 10 μl DT into the solution. The solution was then transferred into a capillary, in which *in situ* SAXS measurements were conducted.

The structural evolution of the NC assemblies with gradual solvent evaporation resulted in the time-dependent development of the SAXS patterns and the corresponding structure factors $S(q)$, as shown in Fig. 2(a). $S(q)$ is

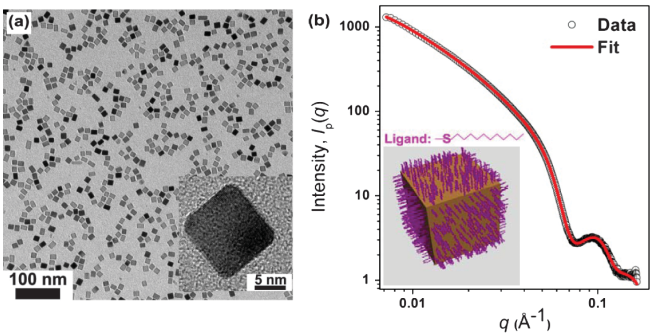

FIG. 1 (color). (a) The TEM image of PVP stabilized Pd nanocubes and (inset) HRTEM image of a Pd cube. (b) SAXS scattering profile obtained from a free NC in a solution (open circles), fit with IRENA2 package (line), and (inset) schematic of a DT-functionalized nanocube, as discussed in the text.

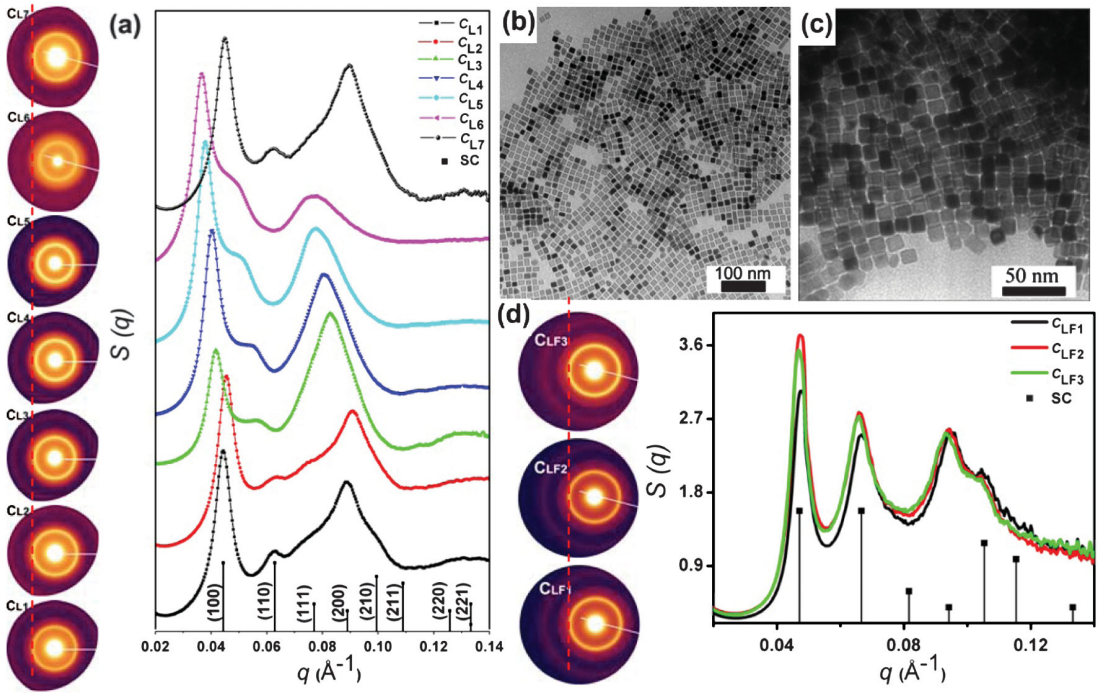

FIG. 2 (color). (a) Evolution of the 2D SAXS patterns and $S(q)$ of assembled nanocubes upon evaporation of ligand-rich solution. The TEM images of nanocubes obtained in the states C_{L1} (b) and C_{L7} (c). (d) $S(q)$ for different states of NC assembly in a ligand-free solution.

obtained as $I_a(q)/I_p(q)$, where $I_a(q)$ and $I_p(q)$ are background corrected SAXS profiles measured from aggregate and free particles, respectively, and peak positions in the $S(q)$ are determined by Lorentzian fitting. We denote q_1, q_2, and q_3 as the positions of the strongest peaks at 0.0444, 0.0628, and 0.0888 Å^{-1}, respectively, for the sample at the initial state (C_{L1}). The sequence of measurements, C_{Ln} ($1 \leq n \leq 6$), corresponds to a sample at 0, 24, 58, 98, 221, and 500 h of evaporation duration at ~370 K, with a solution fully evaporated for C_{L6}.

Based on $S(q)$ analysis we indexed the initial state C_{L1} as a simple cubic (SC) structure [Fig. 2(a)]. Such a SC structure has been previously shown for assemblies of nanocubes [16]. Upon solvent evaporation, SAXS reveals two major structural changes: (i) q_1, corresponding to the (100) plane, shifts towards smaller q from C_{L2} to C_{L6}, and (ii) the peak position ratio q_2/q_1 decreases. Moreover, the second peak, nominally arising from the SC (110) plane, gradually merges into the (100) peak and becomes its shoulder peak. These observations indicate a phase transformation upon solvent evaporation. The NC assembly reversibly transforms into the original SC structure, C_{L1}, from the dried state C_{L6} by adding solvent, as indicated by $S(q)$ for C_{L7}. To investigate the determining factors for the phase evolution, we conducted two control experiments. We first employed TEM to verify the structural stability of the NCs during the solvent evaporation. Figures 2(b) and 2(c) show NCs of similar sizes, shapes, and packing at C_{L1} and at C_{L7}, respectively. Second, analogous experiments without free DT in the solution [denoted as C_{LF} series, Fig. 2(d)] show the stable SC phase for C_{LF1}, C_{LF2}, and C_{LF3}, obtained after 0, 58, and 500 h of evaporation, respectively. Therefore, we conclude that the evaporation-assisted phase transformation is due to the ligand excess, although the local concentration of the ligand in the cube's proximity might differ significantly from an average solution value.

The continuous structural evolution can be described as a gradual distortion of a SC lattice in the [111] direction, which is an angle-variable rhombohedral structure (RS). With an angle α change from 90° to 60°, RS depicts a continuous phase transformation from SC to fcc. This type of transformation has been observed in an arsenic atomic system [17] and porous silica film [18]. The reduced position of the diffraction peak (hkl) for a RS can be expressed as $q(hkl)/q(100) = [(h^2 + l^2 + 2k^2)\sin^2\alpha + 2(hk + kl + lh)(\cos^2\alpha - \cos\alpha)]^{-1/2}\sin^{-1}\alpha$, and the calculated values for $q(110)/q(100)$, $q(200)/q(100)$, and $q(210)/q(100)$ against α are plotted in Fig. 3(a) (solid lines). The planes (100), (110), (200), and (210) of SC phase evolve, respectively, into (111), (200), (222), and (311) of fcc phase when α decreases to 60°. One feature of the RS model is that the $q(110)$ approaches the $q(100)$ gradually with α decrease, which resembles the observed q_2/q_1 evolution for the C_{Ln}. We used experimental values of q_2/q_1 for $q(110)/q(100)$ in the RS model to determine α, then we mapped each C_{Ln} and C_{LFn} on the $q(110)/q(100)$ line in Fig. 3(a) (black symbols). Using the

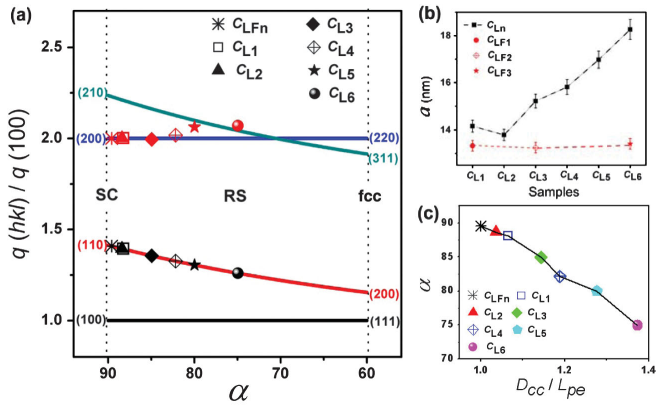

FIG. 3 (color). (a) Calculated ratios of diffraction peak positions for shown planes in SC and fcc phases, and their dependence on α in RS model (lines). Estimated α for assembled phase for different states, from experimental q_2/q_1 ratio (black symbols), and q_3/q_1 values (red symbols) for obtained α. The same black and red symbols correspond to the same sample states. (b) The dependence of a on a system state. (c) The dependence of α on nearest-neighbor NC center-to-center distance (D_{cc}) normalized by effective particle edge length (L_{pe}).

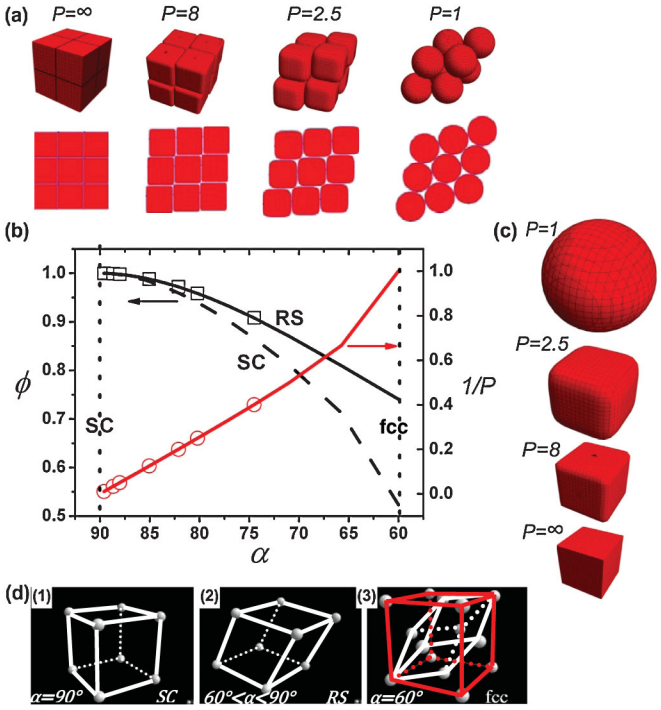

FIG. 4 (color). (a) 3D and 2D illustrations of a phase transformation from SC to fcc via RS phase due to evolution of effective particle shape from cube to sphere using superball model for shown p values. (b) Calculated $1/p$ (red solid line) and ϕ for RS (black solid line) and SC (black dashed line) as a function of α. The black and red symbols correspond to the experimental data, obtained as discussed in the text. (c) Calculated particle shapes as for shown p values. (d) Schematics of the transformation of SC to fcc lattice via RC phase (NCs are represented by white spheres).

obtained α, we plotted q_3/q_1 values [Fig. 3(a), red symbols]. While for all C_{LF} systems, $\alpha \sim 90°$ [Fig. 4(d1)], for the C_L system, α decreases from 88.2° at C_{L1} to 74.9° at C_{L6} [Fig. 4(d2)]. This indicates that a full evolution toward the fcc phase [Fig. 4(d3)] is not completed. The change of a lattice constant a can be estimated for the RS as $a = d(100)\sin\alpha(1 - 3\cos^2\alpha + 2\cos^3\alpha)^{-1/2}$ [Fig. 3(b)]. During solvent evaporation a slightly decreases to 13.8 nm at C_{L2} from 14.2 nm at C_{L1}, possibly due to chain rearrangements, and then it continuously increases, reaching 18.3 nm at C_{L6}.

Based on shape considerations, nanocubes favor the SC phase [16], while fcc packing is preferable for spheres. Thus, we suggest that the α-variable RS phase transformation is related to the system's attempt to accommodate a changing particle shape from a cube to a quasisphere due to a ligand adsorption. The shape evolution results from cohesive interactions between adsorbed and NC-attached DT molecules, and stronger NC-DT van der Waals (vdW) attraction compared to DT-DT. The convex growth of a DT crownlike layer leads to the quasispherical shape transformation of NCs and satisfies the requirement for surface energy minimization [19,20]. Figure 3(c) shows the monotonic increase of α with $x = D_{cc}/L_{pe}$, where D_{cc} is a nearest-neighbor NC center-to-center distance and L_{pe} is an effective NC edge length. For RS $D_{cc} = a$, and $L_{pe} = 13.3$ nm accounting for DT molecule interpenetration [14]. The values of $x = 1$, $\alpha = 90°$ and $x = \sqrt{3}$, $\alpha = 60°$, respectively, correspond to cubes and spheres. For our system we observed a variation of x from 1 to ~1.37, with related a α change from 90° to 74.9°, indicating an incomplete transition from cubes to spheres. A "superball" model [21] with object shape defined by $|x|^{2p} + |y|^{2p} + |z|^{2p} \leq 1$, where x, y, and z are Cartesian coordinates, was introduced to describe the sphere to cube evolution with a shape deformation parameter p change from 1 to ∞, respectively [Fig. 4(c)].

In the framework of the superball model the relationship between a particle shape and a lattice structural response can be established. Interestingly, the densest proposed [21] packing C_1 ($p > 1$) corresponds to a RS with the lattice vectors (L_v) defined as $\boldsymbol{e}_1 = -2(s + 2^{-1/2p})\boldsymbol{i} + 2s\boldsymbol{j} + 2s\boldsymbol{k}$, $\boldsymbol{e}_2 = -2s\boldsymbol{i} + 2s\boldsymbol{j} + 2(s + 2^{-1/2p})\boldsymbol{k}$, $\boldsymbol{e}_3 = -2s\boldsymbol{i} + 2(s + 2^{-1/2p})\boldsymbol{j} + 2s\boldsymbol{k}$, where i, j, k are unit vectors along x, y, and z directions, and s is the smallest positive root of the equation $(s + 2^{-1/2p})^{2p} + 2s^{2p} - 1 = 0$. The L_v construction relates α and p, as $\alpha(p) = \arccos[\boldsymbol{e}_i \cdot \boldsymbol{e}_j/(|\boldsymbol{e}_i||\boldsymbol{e}_j|)]$, $i, j = 1, 2, 3$ ($i \neq j$). Conversely, p is only defined by α as well. The proposed RS mechanism for a lattice transformation is in accord with a local requirement for a particle "sliding" without substantial rotation, which is limited by a particle cusp for $p \neq 1$. We plotted the calculated values of $1/p$ as a function of α [Fig. 4(b), red solid line] and mapped (red circles) corresponding $1/p$ values, from

0 to 0.4, for each experimental α [Fig. 3(c)]. Figure 4(a) illustrates the phase transformation in 3D and its 2D analog from SC to fcc via RS, as induced by evolution of cubes to spheres with shape defined by the superball model. Our measurements shows that the transformation is accompanied by ~40% decrease of a correlation length ξ, reflecting an order diminishment. The Williamson-Hall slope [22], a relative measure of a strain-induced average lattice distortion, increases nearly 50 times for a corresponding $1/p$ change from 0 to 0.4, indicating a strain growth, a possible origin of ξ decrease. We note that a decreased local mobility of NCs due to the solvent evaporation can be responsible for the incomplete RS to fcc transformation and the strain increase. A full evolution to spheres is hindered when the ligand shell increases: convex DT layer growth is decreased, and the adsorption of DT molecules on a NC is diminished due to the reduction of vdW interaction.

The shape-induced phase transition is advantageous considering packing efficiency and interparticle interactions. To evaluate a favorable packing, we calculated volume fractions, $\phi(p)$, occupied by particles in RS and SC phases, as $\phi_{\mathrm{RS}}(p) = V_{\mathrm{sb}}(p)/V_{\mathrm{RS}}(p)$ and $\phi_{\mathrm{SC}}(p) = V_{\mathrm{sb}}(p)/V_{\mathrm{SC}}(p)$, respectively, where V_{sb} is the volume of superball [21], and $V_{\mathrm{RS}}(p) = \boldsymbol{e}_1 \times \boldsymbol{e}_2 \cdot \boldsymbol{e}_3$ and $V_{\mathrm{SC}}(p) = \boldsymbol{e}_1 \times \boldsymbol{e}_2 \cdot \boldsymbol{e}_3|_{p=\infty} = 8$ are the unit cell volumes of RS and SC, respectively. The calculated ϕ_{RS} and ϕ_{SC} [Fig. 4(b), black solid and dashed lines] show that the difference in ϕ between RS and SC for $1/p < 0.05$ is very small; however, it quickly increases for $1/p > 0.12$. This indicates that RS offers a denser packing than SC for rounded particles, which justifies the SC to RS transition with $1/p$ increase, while ϕ_{RS} also exhibits the densest known packing of rounded cubes [21]. The higher packing for RS compared to SC is intuitively easy to understand: by allowing for an α-dependent cube sliding RS provides offset for the highest points on the convex surfaces of adjacent rounded cubes. The recent theoretical work [23] shows that rounded cubes can pack in a less dense cubatic phase for about $1/p > 0.4$; however, such a degree of roundness is not realized in our system. From the interaction point, we consider solely the vdW forces between NCs. Because of their short range character, only interaction between adjacent particles (W_a) is included [16]. When $1/p$ increases from 0 to 0.12, W_a decreases quickly from $\sim 14 k_B T$ to $\sim 4 k_B T$, and $W_a \sim k_B T$ for $1/p > 0.25$. Therefore, for a small $1/p$ (cubelike) a face-to-face SC arrangement of ligand coated NCs is also favorable from vdW consideration, since a center-to-center distance is minimized. vdW interactions become less significant when particle shape evolves toward a quasisphere ($1/p$ increase), which favors a RS transformation.

In summary, we investigated the relationship between nanoparticle shape, ligand shell, and the emergent phase behavior of nanocube assemblies. The observed RS phase transformation was attributed to the evolution of a particle's shape from a cube to a quasisphere due to the ligand adsorption with the densest known pathway.

Research was supported by the U.S. Department of Energy, Basic Energy Sciences, Materials Sciences and Engineering Division. Research was carried out at the Center for Functional Nanomaterials and the National Synchrotron Light Source, Brookhaven National Laboratory, supported by the U.S. Department of Energy, Office of Basic Energy Sciences, under Contract No. DE-AC02-98CH10886.

*Current address: Center for Agricultural and Environmental Biotechnology, Research Triangle Institute International, Research Triangle Park, NC 27709-2194, USA.

†ogang@bnl.gov

[1] B. A. Korgel and D. Fitzmaurice, Phys. Rev. Lett. **80**, 3531 (1998).
[2] H. M. Xiong, D. van der Lelie, and O. Gang, Phys. Rev. Lett. **102**, 015504 (2009).
[3] D. Pontoni *et al.*, Phys. Rev. Lett. **102**, 016101 (2009).
[4] A. Donev *et al.*, Phys. Rev. Lett. **92**, 255506 (2004).
[5] K. Liu *et al.*, Science **329**, 197 (2010).
[6] X. Zhang, Z. L. Zhang, and S. C. Glotzer, J. Phys. Chem. C **111**, 4132 (2007).
[7] R. P. A. Dullens *et al.*, Phys. Rev. Lett. **96**, 028304 (2006).
[8] M. R. Jones *et al.*, Nature Mater. **9**, 913 (2010).
[9] S. Narayanan, J. Wang, and X. M. Lin, Phys. Rev. Lett. **93**, 135503 (2004).
[10] T. Ming *et al.*, Angew. Chem., Int. Ed. **47**, 9685 (2008).
[11] T. D. Nguyen and S. C. Glotzer, ACS Nano **4**, 2585 (2010).
[12] M. M. Maye *et al.*, Nature Nanotech. **5**, 116 (2009).
[13] B. Lim *et al.*, Adv. Funct. Mater. **19**, 189 (2009).
[14] L. Motte, F. Billoudet, and M. P. Pileni, J. Phys. Chem. **99**, 16 425 (1995).
[15] J. Ilavsky and P. R. Jemian, J. Appl. Crystallogr. **42**, 347 (2009).
[16] S. Yamamuro and K. Sumiyama, Chem. Phys. Lett. **418**, 166 (2006).
[17] T. Kikegawa and H. Iwasaki, J. Phys. Soc. Jpn. **56**, 3417 (1987).
[18] B. W. Eggiman, M. P. Tate, and H. W. Hillhouse, Chem. Mater. **18**, 723 (2006).
[19] P. G. de Gennes, F. Brochard, and D. Quéré, *Capillarity and Wetting Phenomena Drops, Bubbles, Pearls, Waves* (Springer, New York, 2003), Chap. 7, p. 153.
[20] A. Checco, O. Gang, and B. M. Ocko, Phys. Rev. Lett. **96**, 056104 (2006).
[21] Y. Jiao, F. H. Stillinger, and S. Torquato, Phys. Rev. E **79**, 041309 (2009).
[22] G. K. Williamson and W. H. Hall, Acta Metall. Mater. **1**, 22 (1953).
[23] R. D. Batten, F. H. Stillinger, and S. Torquato, Phys. Rev. E **81**, 061105 (2010).